RSC Advances

PAPER

View Article Online
View Journal | View Issue

Cite this: *RSC Adv.*, 2025, **15**, 13188

Recovery of cellulose nanocrystal from mixed office wastepaper and the development of bio-based coating matrixes with enhanced water, gas, oil, and grease resistances for packaging

Anik Baral,†[a] Niloy Roy Kerjee,†[a] Nazia Afrin Jashi,[bc] Md. Ismail Hossen Emon,[a] Munmun Basak,[c] Md. Mostafizur Rahman,[d] A. F. M. Mustafizur Rahman,[a] Mohammed Mizanur Rahman,[a] Lokendra Pal,[c] Mohammad Shahruzzaman[a] and Khandoker Samaher Salem *[a]

This study on sustainable nanocellulose modifications for various packaging applications is driven by the global social awareness and growing demand for bioproducts to reduce the use of single-use plastics. Mixed office waste (MOW) was used as the raw material to extract cellulose nanocrystals (CNCs) *via* the acid hydrolysis method. The average length and diameter of the CNCs were approximately 104.08 ± 0.1 nm and 9.49 ± 0.3 nm, respectively. The crystallinity index was 87%, as confirmed using transmission electron microscopy and X-ray diffraction analysis. Coating solutions of varying concentrations were prepared by mixing CNCs with collagen hydrolysate and glycerin, and the coatings were applied to the surface of uncoated paper *via* a rod coating process. FTIR spectra confirmed the presence of CNCs in the coated paper. High-resolution FE-SEM images provided detailed information on the surface morphology of the coated papers. The barrier and mechanical performances of the coated paper were evaluated using the oil and grease resistance KIT, hot oil, water vapor permeability, air permeability, water contact angle, tensile index, burst index, percentage of elongation, and fold tests. All the coated paper samples passed the hot oil test and exhibited the highest KIT rating. The water vapor and air resistance values of the coated paper samples increased 14 times and 250 times, respectively, compared with the uncoated paper samples. The water contact angle of the coated paper samples increased to 99.40° from 60.13°, and the surface roughness decreased from 2.37 μm to 0.85 μm. The presence of coating also increased the tensile and burst indices by 5.28 times and 1.79 times, respectively, compared with the uncoated paper samples. No cytotoxic effects were found in the optimized coated paper, and all the samples were fully degraded within 49 days, as confirmed using the soil biodegradability test. Therefore, the coated paper can be a potential alternative to existing single-use plastics for packaging materials.

Received 3rd March 2025
Accepted 28th March 2025

DOI: 10.1039/d5ra01516b

rsc.li/rsc-advances

1 Introduction

Packaging plays a critical role in the field of product supply chain management. The primary function of packaging is to protect the products from external factors, such as dust, moisture, chemical pollution, microbial contamination, and volatile substances, while preventing physical damage during transportation in all logistic phases.[1–3] In the past few decades, plastic packaging has replaced traditional packaging materials, such as cardboard, metal, and paper, owing to its lightness, cost-effectiveness, compatibility, and ease of production.[4,5] Most plastics are produced from petroleum, and their long-term degradation leaves detrimental effects on the environment.[6] Nondegradable plastics accumulate in the environment, generate secondary microplastics and nano-plastics, and release hazardous chemicals while manufacturing. The extensive use of plastic and its improper disposal and combustion lead to environmental pollution.[7–10] Poor plastic waste management can cause drain clogging in cities and surrounding areas.[11] Approximately 10–12% of plastic residues from municipal solid waste is combusted, releasing greenhouse gases into the environment. As a result, air pollution increases,

[a]*Applied Chemistry and Chemical Engineering, University of Dhaka, Bangladesh. E-mail: samaher.salem@du.ac.bd*

[b]*Institute of Leather Engineering and Technology, University of Dhaka, Bangladesh*

[c]*Department of Forest Biomaterials, North Carolina State University, 431 Dan Allen Dr., Raleigh, NC 27695-8005, USA*

[d]*Pulp and Paper Research Division, Bangladesh Council of Scientific and Industrial Research, Dhaka, Bangladesh*

† Co first author.

contributing to the greenhouse effect.[5,11] At the turn of the 21st century, owing to the depletion of petroleum resources and the emergence of environmental problems, biodegradable and bio-based packaging gained increased attention as a replacement for plastic packaging. Hence, the world is currently moving towards naturally derived bio-based packaging materials to replace plastic packaging products.[12,13]

Bio-based packaging materials are derived from renewable sources, which results in a lower carbon footprint, less environmental impact,[14] waste management,[15,16] more customer acceptability, preservation of the packed good's barrier qualities and shelf life, and sustainable end-of-life management.[17] Many companies, including PepsiCo, Kraft Heinz, and McDonald's, have recently announced plans to shift toward completely biodegradable packaging with 100% renewable and recyclable materials by 2025.[18,19] In 2022, Eurostat data show that Europeans generated 83.4 million tons of packaging waste, equivalent to 186 kg per inhabitant. The share of plastic packaging waste, paper and cardboard, glass, wood, and metal was 19.4%, 40.8%, 18.8%, 16%, and 4.9%, respectively. Wastepaper, being a valuable resource for extracting cellulose, can be chemically modified to produce economically significant cellulose derivatives, as well as a variety of environmentally friendly and useful specialty end products.[20,21] Wastepaper from office waste is an economic resource to produce CNCs. Mixed office waste (MOW) includes phone books, old mail, paperboard, and daily office paper waste that are recycled to produce products such as tissues, chipboard, wallboard, and cellulose insulation through the pulping and deinking process.[22,23] However, this production is less economically feasible than virgin pulp production. The biggest challenge in the recycling processes of MOW is reducing the cellulose fiber length, which results in weaker and lower-quality paper products than those made from virgin pulp.[24]

Wastepaper recycling results in shorter fiber lengths of cellulose, which leads to poor-quality paper. Since the highest percentage of paper-to-paper recycling is 65%,[25,26] enormous amounts of byproducts are produced, which must be disposed of eventually. With the rising expense of generating paper from recycled paper and the disposal of waste fibers that are unfit for use, the development of new techniques to recycle wastepaper is essential. Due to its cellulosic composition, wastepaper can be used as a raw material in the manufacturing of CNCs. Manufacturing CNCs from wastepaper would give an alternative to paper recycling while potentially addressing the issue of byproduct generation from paper-to-paper recycling.[1,27] In the past decade, cellulose nanomaterials have garnered significant interest due to their lightweight nature, low cost, ease of recycling, and environmental friendliness.[28,29] The ecotoxicity of nanocellulose is very low.[30,31] CNCs are used in packaging as a filler[32,33] and reinforcing agents in polymeric matrices due to their strength, high aspect ratio, surface area, and high tensile modulus.[34] CNCs can form hydrogen bonds that create a dense and strong network within the packaging material, preventing the permeation of various molecules through the packaging layers and thereby increasing the barrier properties.[35,36]

The main motive of the present work was to upcycle MOW by extracting CNCs from it through an acid hydrolysis process. A coating recipe was developed using CNCs from recycled sources, collagen hydrolysate, and glycerin, and was applied as a coating on paper to evaluate its barrier and mechanical properties. The work emphasizes upcycling waste paper while contributing to environmental sustainability. The findings explore the potential of recycled, biodegradable materials as promising alternatives to conventional non-biodegradable single-use plastics.

2 Experimental sections

2.1 Materials

Mixed office waste (MOW) and brown uncoated base paper (100 g m^{-2}) were collected from the local market. Collagen hydrolysate was extracted from shaving dust collected from the local tannery industry, a procedure established in our laboratory.[37] Sodium sulfate (Na_2SO_4, lab grade, >99% purity), sodium carbonate (Na_2CO_3, lab grade, >99.5% purity), sodium hydroxide (NaOH, lab grade, 1 M), glacial acetic acid (CH_3-COOH, lab grade, 99% purity), concentrated sulfuric acid (H_2SO_4, lab grade, 98%) and glycerin were purchased from Merck, Germany. Hydrogen peroxide (H_2O_2, technical grade, 70% purity) was purchased from Research-Lab Fine Chemical Industries, India.

2.1.1 Preparation of cellulose nanocrystals. MOW was soaked in water overnight. Pulp was made from these materials using a Valley beater under full load. The MOW pulp was used as a raw material to produce cellulose nanocrystals (CNCs). The composition of MOW was cellulose-72.49%, hemicellulose-13.73%, lignin-3.65%, ash-6.29%, and moisture-3.84%. First, 2 g of pulp obtained from MOW was taken in a container, and 20 mL of H_2SO_4 (50% v/v) was added. The container was sealed carefully through a sealer machine. Then it was dipped into a water bath at 45 °C for 1 h. Then, the sample was transferred into a falcon tube for washing through a centrifuge to neutralize the pH of the solution. After washing several times, the sample was transferred into a beaker, and a drop of phenolphthalein indicator and 2 mL of 0.1 M NaOH solution were added to neutralize the solution completely. The neutralized suspension was mechanically treated using a high-speed disperser (T-18 digital ULTRA-TURRAX) operating at 20 000 rpm for 30 minutes. Finally, the sample was transferred into a cyclone separator and kept for 24 h to settle down. Residue was collected from the bottom, and the suspension from the upper section containing nanocellulose was further centrifuged to remove water content. The final product contained CNCs in the form of suspension. Fig. 1 represents the extraction process of CNCs from mixed office waste (MOW).

2.2 Formulation of the coating recipe

A 10% collagen hydrolysate solution was prepared by dissolving collagen hydrolysate powder in 1% acetic acid solution and 0.5–1 mL of glycerin. Then, 1, 3, 5, 7, and 10% of CNCs were taken in the weight ratio of the collagen hydrolysate powder. The formulations were prepared following Table 1 by stirring for 24 h at room temperature and sonicated for 20 min to remove

Fig. 1 CNC extraction from mixed office waste (MOW).

Table 1 Coating formulations with collagen hydrolysate, CNCs and glycerin

Serial no.	Coating recipes	Sample ID
1	Uncoated base paper	UP
2	Paper coated with 1% CNCs, 10% collagen hydrolysate, and (0.5–1) mL of glycerin	CP-1%
3	Paper coated with 3% CNCs, 10% collagen hydrolysate, and (0.5–1) mL of glycerin	CP-3%
4	Paper coated with 5% CNCs, 10% collagen hydrolysate, and (0.5–1) mL of glycerin	CP-5%
5	Paper coated with 7% CNCs, 10% collagen hydrolysate, and (0.5–1) mL of glycerin	CP-7%
6	Paper coated with 10% CNCs, 10% collagen hydrolysate, and (0.5–1) mL of glycerin	CP-10%

the bubbles. Fig. 2 represents the application steps of CNC-based coating on the packaging material.

2.2.1 Coating solution application by rod coating. A coating solution of the desired amount was applied on the uncoated base paper through rod coating by using Meyer rod no. 12 to get the desired coat weight of 35 g m^{-2}, and the resulting coating thickness was 0.03 mm. After coating application, the coated papers were dried by hot air flow and conditioned for 24 h at a TAPPI (T402 sp-98) standard conditioning temperature of 23 °C and 50% relative humidity (RH) before testing.

2.3 Characterization

2.3.1 X-ray diffraction (XRD). The characteristics of the CNCs were observed from the diffraction patterns obtained by the X-ray diffraction method. The X-ray diffractometer (RIGAKU ULTIMA IV X-ray Diffractometer, Japan) used for sample analysis consisted of a radiation source of Cu Kα operating at 8.04 kV. The samples were analyzed at a diffraction angle (2θ) from 5° to 40° at room temperature. The wavelength of the X-ray was 1.5406 Å, and the step rate was 3° min^{-1}. The crystallinity index of CNCs was determined by the Segal peak height method, using the following formula:[38]

$$\text{Crystallinity index (CI)} = 100 \times (I_{200} - I_{\text{am}})/I_{200} \quad (1)$$

According to the equation, the Segal technique[39] was used to determine the crystallinity index (CI) from the heights of the (200) peak (I_{200}, $2\theta = 22.6°$) and the minimum intensity between the (200) and (110) peaks (I_{am}, $2\theta = 18°$). I_{am} stands for the

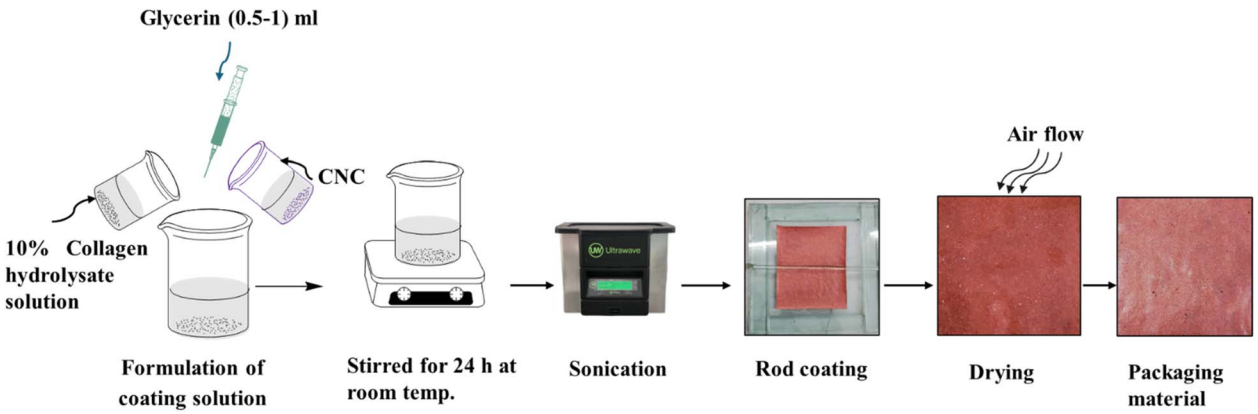

Fig. 2 CNC-coated paper as a packaging material.

amorphous material, while I_{200} denotes both crystalline and amorphous materials.

2.3.2 Transmission electron microscopy (TEM). A Tecnai-12 (Philips) transmission electron microscope running at 120 kV was used to evaluate the size of the CNCs. Low-dose circumstances were used to observe the specimens. A TVIPSF224 CCD camera was used to capture the images.[40] The CNC suspensions were diluted to 100 μg mL^{-1} and sonicated three times for 60 s each with a cold bath before deposition on the grid. Drops (5 μL each) were placed and blotted on glow-discharged carbon-coated copper TEM grids for one minute. The staining was not done.

2.3.3 Fourier transform infrared (FTIR) spectroscopy. FTIR analysis was performed using an IRSpirit-X Series Fourier Transform Infrared Spectrophotometer. The sample was used as a solid without any pretreatment or modifications. The baseline was corrected before the test sample was placed. In this analysis, all spectra were measured after 64 scans per sample from wavenumber 400 to 4000 cm^{-1} with a resolution of 4 cm^{-1}. The FTIR spectra were recorded in the transmittance mode.[41]

2.3.4 Field emission-scanning electron microscopy (FE-SEM). An FE-SEM (SU8700, Hitachi High-Tech Corporation, Japan) was used to investigate the surface and cross-section of the coated and uncoated papers. The micrograph of the composites was taken at an accelerating voltage of 5 kV and a resolution of 20 μm. The samples were kept on a stub with carbon tape and coated with AuPd to obtain better images by applying a thin conductive layer.

2.3.5 Barrier properties measurement. For the grease resistance KIT test, the testing method was TAPPI UM 557, where three organic solvents were used at twelve ratios (KIT no. 1–12). KIT no. 1 was the mildest, and KIT no. 12 was the harshest solution.[42] Both coated and uncoated papers were tested in hot oil barrier tests. A hot oil solution was prepared by mixing red dye (D53004 Chromatint® Red IK Liquid) with one gallon of Mazola corn oil to achieve a 0.1% concentration. The solution was heated to 62–65 °C and poured onto the coated surface at a depth of 3 mm. The sample was left for 20 minutes, and the time was checked with a stopwatch. The oil was removed from the coated surface after 20 minutes, and any excess oil was cleaned using a tissue paper. The backside of the coated paper was immediately observed for soak-through or staining. The uncoated and coated samples were tested for air (Gurley porosity) and water vapor permeability using the T460 om-96 and STM 473 methods, respectively. For water vapor permeability, the diameter of the sample was 34 mm, and the sample was placed in the neck of the holder. The silica gel was rotated for 8 hours, and the sample weight was measured before and after the test. For air permeability, the sample size was 30 mm in diameter and placed in the Gurley apparatus, which was filled with air that was compressed by the weight of a vertical cylinder floating in liquid. In the Gurley porosity tester, air permeability was calculated as a function of the time required for a specific volume of air to pass through a specified area and pressure.

2.3.6 Mechanical properties. The tensile properties of the uncoated and coated papers were evaluated using a universal testing machine (model: STM 566, SATRA, UK). Standardized strip specimens (length, 80 mm; width, 10 mm) were cut into dumbbell shapes from the coated paper at room temperature and 50% relative humidity (RH). The accurate width and thickness of each sample were determined using a slide caliper. The burst index was measured using a lastometer (model: STM 463, SATRA Technology). All paper samples were cut into circular shapes with a diameter of 45 mm, on which the force from a ball plunger was recorded.

2.3.7 Thermogravimetric analysis (TGA). TGA and its first derivative (DTGA) were done using a PerkinElmer model TGA 8000, Netherlands. The experiments were conducted at a temperature in the range of 50 to 620 °C, at a heating rate of 20 °C min^{-1} and a nitrogen flow rate of 20 mL min^{-1}. The samples were placed in pans with a perforated cover, allowing water vapor and other volatile compounds to escape during the thermal breakdown of the coatings.

2.3.8 Water contact angle. The hydrophilicity of the coated paper was studied using a contact angle measuring machine (Attension Theta). The uncoated and coated paper samples were first cut into rectangular specimens with a width of 15 mm and a length of 50 mm. Then, a water droplet was placed on the specimen for 10 seconds. Pictures were taken, and the contact angles were determined using the machine. All the measurements were performed at room temperature.

2.3.9 Surface roughness. A Keyence VKx1100 confocal laser scanning microscope was used to measure the surface roughness. R_z is the average peak-to-valley height and R_a is the arithmetical mean line roughness in the 0.1 μm to 1 mm range.

2.3.10 Cytotoxicity assessment. The Vero cell line, which consists of kidney epithelial cells extracted from African green monkeys, was used to test the cytotoxicity of the medium. The medium contains 1% penicillin–streptomycin (1 : 1), 2% gentamicin, and 10% fetal bovine serum (FBS). Cells (3.0×10^4/200 μL) were seeded into 48-well plates and incubated at 37 °C with 5% CO_2. The following day, 50 μL (autoclaved) samples were added to each well, and after 48 hours of incubation, the cytotoxicity was investigated using an inverted light microscope.

2.3.11 Biodegradability. The biodegradation of the composites was checked by a soil burial test. Samples (UP, CP-3%, CP-5%, CP-7% and plastics such as polypropylene, polystyrene and polyethylene) have undergone biodegradability tests. The samples were cut into 2 cm × 2 cm squares and placed in soil (plantation quality) at a depth of 9 cm, at pH = 7.2 with 50% moisture content, which was checked periodically for the extent of degradation.[43]

3 Results and discussion

Fig. 3A represents the XRD data, where the crystallinity index of CNCs was determined through the Segal peak height method.[39] The crystallinity index of CNCs obtained from mixed office waste (MOW) was 87%. The increase in the crystallinity index (CI) for CNCs was due to the effective removal of non-cellulosic components from the fibers, specifically the dissolution of amorphous regions, through a controlled acid hydrolysis

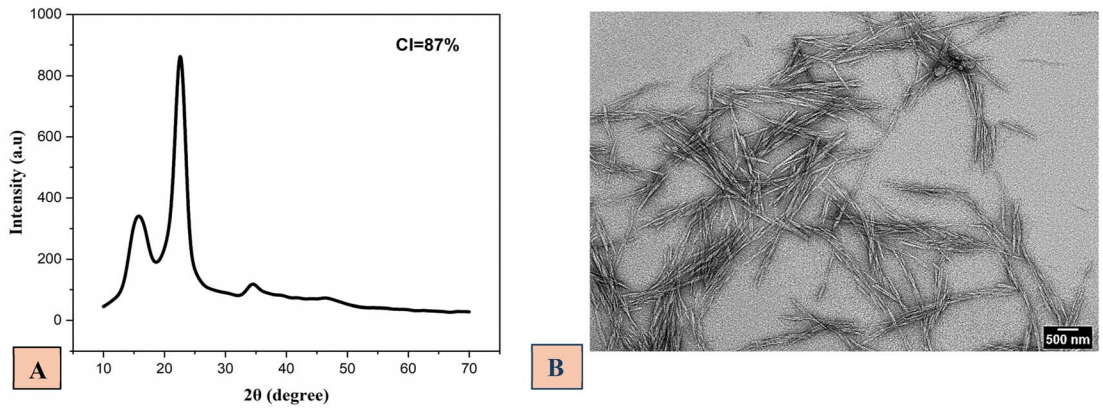

Fig. 3 (A) XRD graph of CNCs. (B) TEM analysis of CNCs obtained from MOW.

process, which accounts for the increased crystalline nature of nanocellulose.[40]

The TEM image shown in Fig. 3B exhibits the morphology of CNC samples. The treated CNC suspension consisted of long, rod-like particles, comprising individual filaments and some agglomerated bundles. The acid hydrolysis process seems to have removed amorphous cellulose and hemicellulose. The average length, diameter, and aspect ratio of CNCs were, respectively, 104.08 ± 0.1 nm, 9.49 ± 0.3 nm, and 10.97 ± 0.2 nm.

The coated and uncoated papers were examined using FTIR, as shown in Fig. 4A. Compared with uncoated paper, new absorption peaks were found for CP-3% at 2955 cm^{-1} for amide, 1659 cm^{-1} for amide I (C═O stretching), 1560 cm^{-1} for amide II (N–H bending), 1268 cm^{-1} for amide III (C–N stretching), 1471 cm^{-1} for $–CH_2$ bending vibration, and 1350 cm^{-1} for C═O stretching vibration due to collagen hydrolysate. Compared with the neat collagen hydrolysate and uncoated paper, the peaks at 1125 cm^{-1} corresponding to collagen and 1029 cm^{-1} corresponding to uncoated paper shifted and formed a new peak at 1096 cm^{-1} because of hydrogen bonding between the –OH group of cellulose and $–NH_2$ and –COOH groups of collagen, ensuring the coating effect of collagen to the uncoated paper.

The FE-SEM images provide detailed information about the morphology of coated and uncoated paper, as shown in Fig. 4B. A smooth surface was observed when the uncoated paper was coated with CP-3%. However, as the concentration of CNCs in the CP-5% coated paper increased, agglomeration occurred

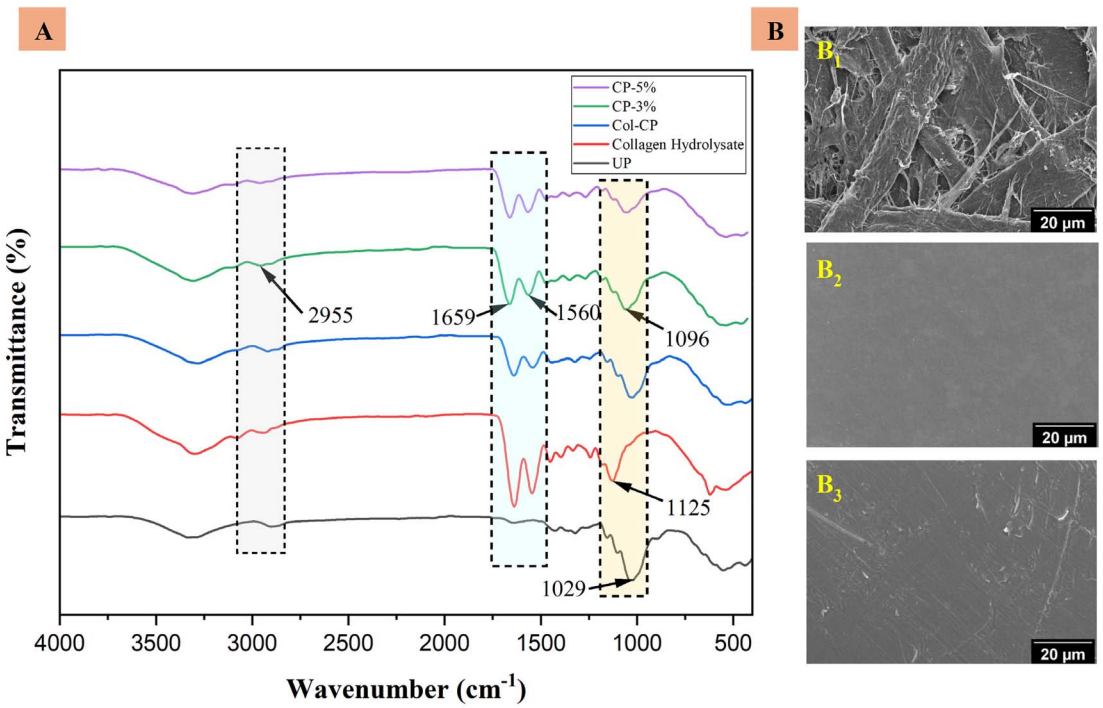

Fig. 4 (A) FTIR spectra of collagen hydrolysate, uncoated base paper and coated paper. (B) FE-SEM image of UP (B1), CP-3% (B2), and CP-5% (B_3).

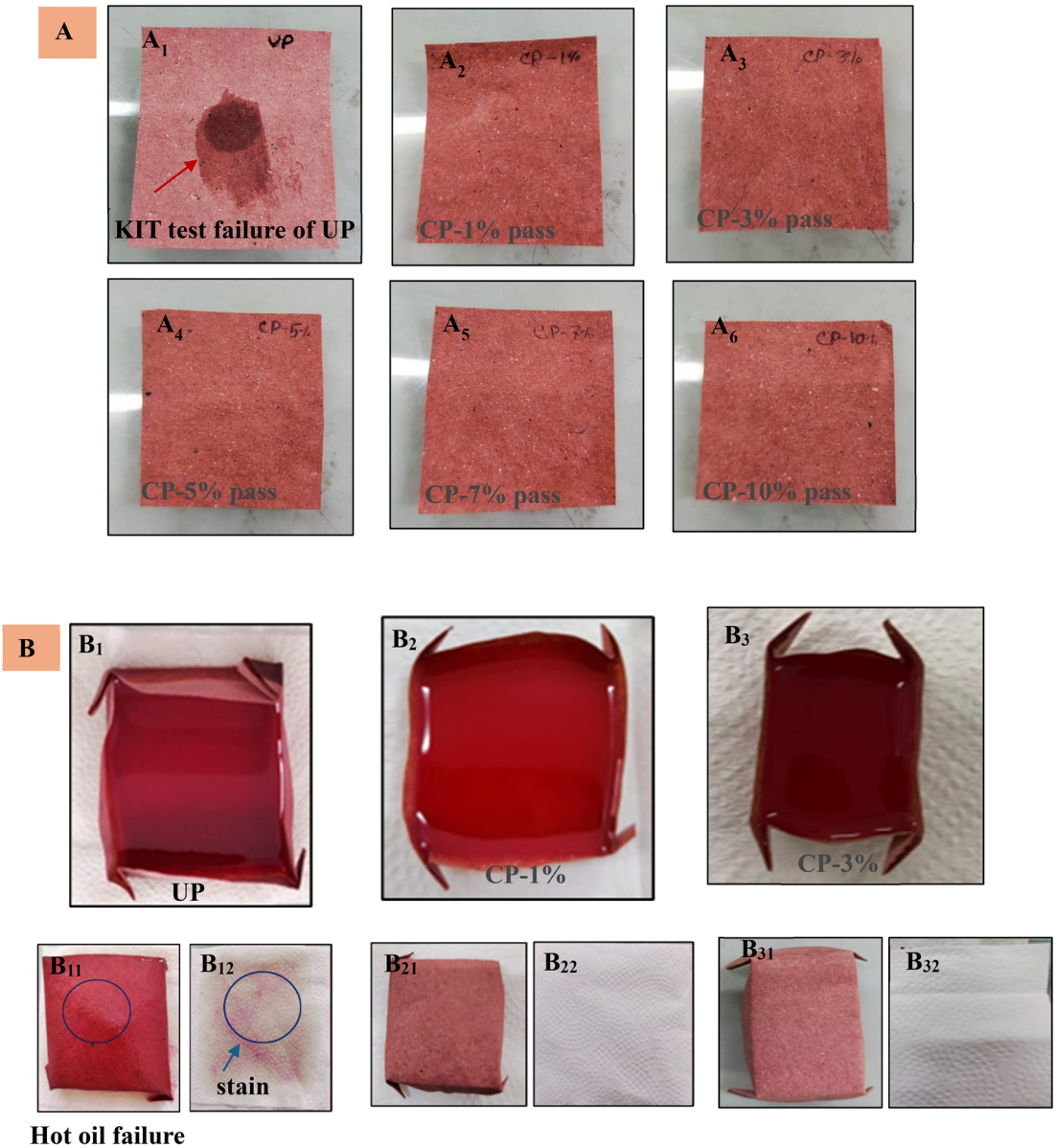

Fig. 5 (A) Oil and grease resistance (KIT) test of UP (A_1), CP-1% (A_2), CP-3% (A_3), CP-5% (A_4), CP-7% (A_5) and CP-10% (A_6) samples, (B) hot oil test of UP (B_1), CP-1% (B_2), and CP-3% (B_3) samples, and observations of the backside of the papers (B_{11}, B_{21}, and B_{31}) and underneath of the tissue paper (B_{12}, B_{22}, and B_{32}).

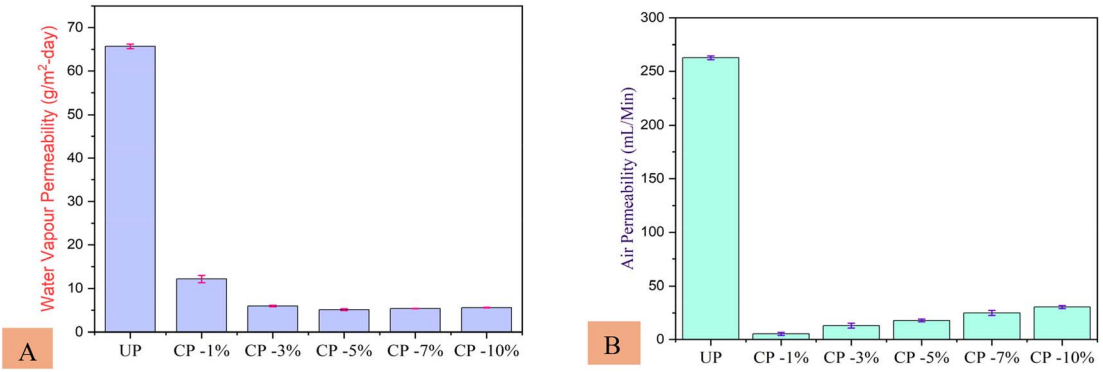

Fig. 6 (A) Water vapor permeability and (B) air permeability of uncoated and coated papers.

between the CNC particles, which reduced the uniformity of the coating layer on the paper.

Grease resistance KIT tests were also conducted on coated and uncoated paper samples using 12 different oil and grease concentrations, as specified in the TAPPI standard. In Fig. 5A, the uncoated base paper (UP) failed to pass KIT rating 1, whereas the coated paper samples (CP-1%, CP-3%, CP-5%, CP-7%, and CP-10%) passed the highest KIT rating 12, indicating better oil and grease resistance. Oil and grease are nonpolar substances, whereas CNCs and glycerol have polar hydroxyl groups that do not interact with nonpolar oil and grease. As a result, all the coated papers have oil and grease-repellent properties. Fig. 5B represents the hot oil test, which was performed to evaluate the oil barrier properties of both coated and uncoated papers, and the results are shown in Fig. 5B. The uncoated base paper (UP) failed the hot oil test. Still, all the coated papers passed the hot oil barrier test. Red stains were seen on the surface of UP and the tissue paper under it. No stains were observed on the surface of the coated paper or under its tissue papers because of the uniform coating and oil repellency of the CNC-based coating.

In water vapor transmission and air resistance tests, the coated paper exhibited higher barrier properties than the uncoated paper due to its smooth coating surface, on which

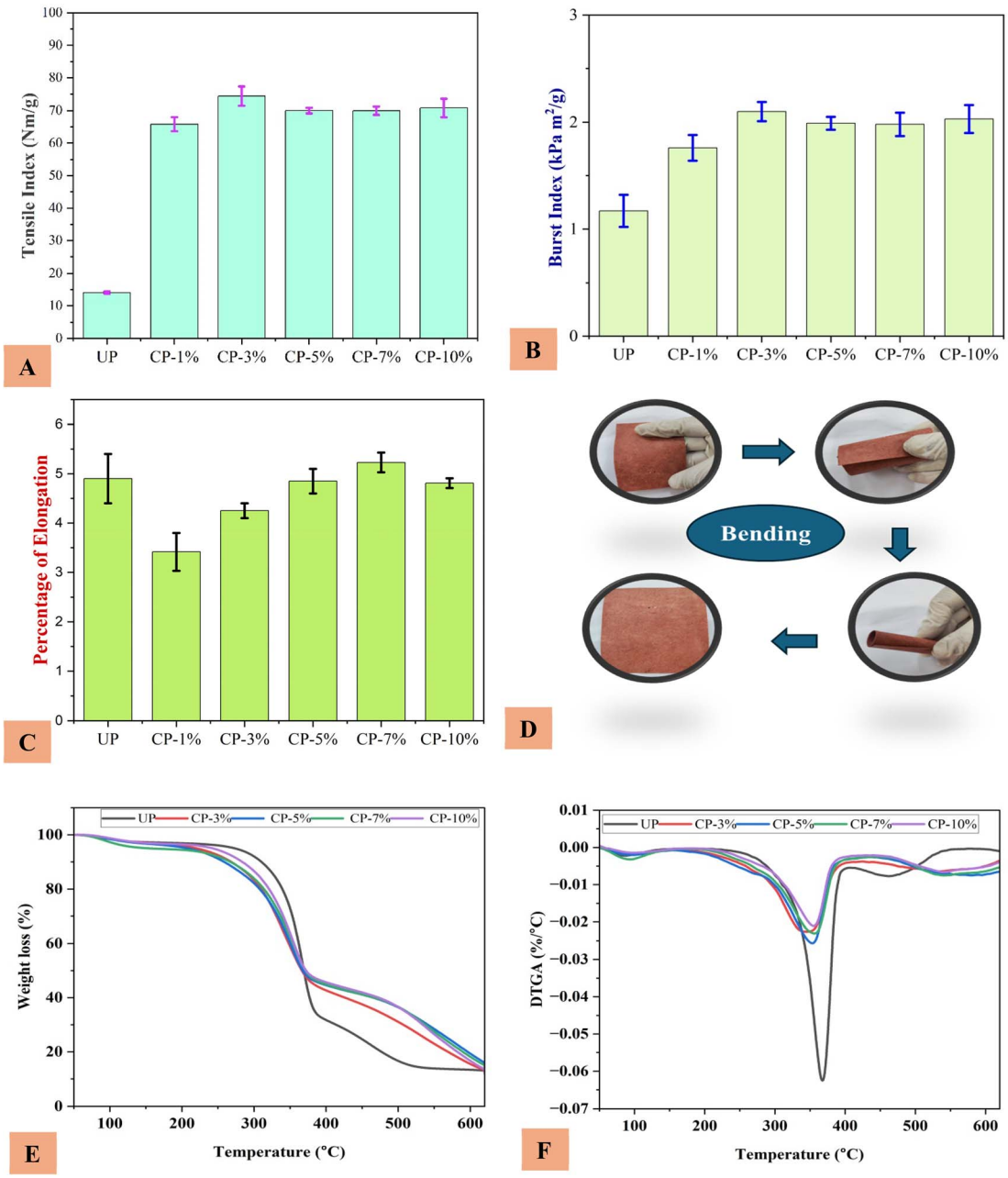

Fig. 7 (A) Tensile index, (B) burst index, and (C) elongation at break of uncoated and coated papers. (D) Depiction of the bending property of coated paper, (E) TGA, and (F) DTGA of uncoated and coated papers, showing their thermal behaviors.

CNCs were dispersed homogeneously. Here, the CNC-based coating acted as a reinforcement filler, decreasing the air permeability of the paper and forming a dense, compact structure through the penetration of cellulose crystals into the cellulose matrix of the paper, which resulted in strong hydrogen bonding. The decrease in water vapor permeability of the coated paper was attributed to the blocking of fiber gaps by CNCs and the hydrophobic properties of the collagen hydrolysate. However, as the percentage of CNCs increased, the value of water vapor resistance did not change much. Almost similar values for CP-5%, CP-7%, and CP-10% are shown in Fig. 6A. The air permeability values of coated paper samples incorporating different concentrations of CNCs are illustrated in Fig. 6B. The coated paper showed higher air barrier properties than uncoated paper. The higher porosity and air permeability of uncoated base paper were due to the presence of large pores, as shown in Fig. $4B_1$. Coated paper formed a dense, compact structure with CNCs, collagen hydrolysate, and glycerin on the surface of the uncoated-based paper, which provided a more tortuous pathway for the diffusion of air molecules and enhanced the air barrier performance.

The mechanical properties of packaging materials were evaluated to determine their stability and strength during handling, transportation, and storage of products in packaging. The tensile index and burst index of samples were measured, as shown in Fig. 7A and B. The coated paper CP-3% exhibited the highest tensile and burst index values due to the addition of CNCs, which reinforced the uncoated paper by making the polymers with a cellulose matrix more rigid and compact. The enhanced mechanical properties are due to increased interaction between the OH groups of CNCs and the available groups (COOH, NH_2, $C(NH_2)_2$, and $CONH_2$) of collagen hydrolysate with the OH group of cellulose of uncoated paper. For the CP-3% coating sample, the ultimate tensile index was 74.43 $\pm$ 2.895 N m g^{-1}, which was 5.28 times higher than that of the UP sample (14.10 $\pm$ 0.315 N m g^{-1}). The burst index for the CP-3% coating sample was 2.10 $\pm$ 0.09 kPa m^2 g^{-1}, which was 1.79 times higher than that of the UP sample (1.17 $\pm$ 0.15). The tensile and burst indexes decreased slightly for coated paper samples (CP-5%, CP-7%, and CP-10%) due to the agglomeration of CNCs at increased concentrations, resulting from non-uniform coating. Fig. 7C shows that the percentage of elongation decreased in CP-1% and then slightly increased due to the presence of CNC content in the coating. The presence of CNCs and collagen on the paper did not significantly impact the elongation. Fig. 7D depicts the bending properties of the coated paper, where no crease was observed due to folding or stretching, as the presence of coating added flexibility to the coated paper.

TGA and DTGA were used to depict the thermal behavior of uncoated and coated papers over a temperature range of 50–620 °C. The incorporation of CNCs and collagen hydrolysate into uncoated paper resulted in a delay in the mass loss of the coated papers within the temperature range (Fig. 7E). The DTGA curves for coated papers (Fig. 7F) showed less degradation of the CP-3%, CP-5%, CP-7%, and CP-10% samples than the uncoated papers. This could be related to the strong interactions between the cellulosic matrix of the paper and the coating solution, as identified by FTIR spectroscopy (Fig. 4A).

The hydrophilic properties of the uncoated base paper (UP) and coated paper samples were measured using the water contact angle (WCA), as shown in Fig. 8A. The WCA of UP was found to be 60.13° due to the porosity of the paper and higher interaction of the cellulosic matrices and water hydroxyls. In Fig. 8B, the WCA of CP-1% and CP-3% gradually increased from 69.25° to 99.40° because of the hydrophobic properties of

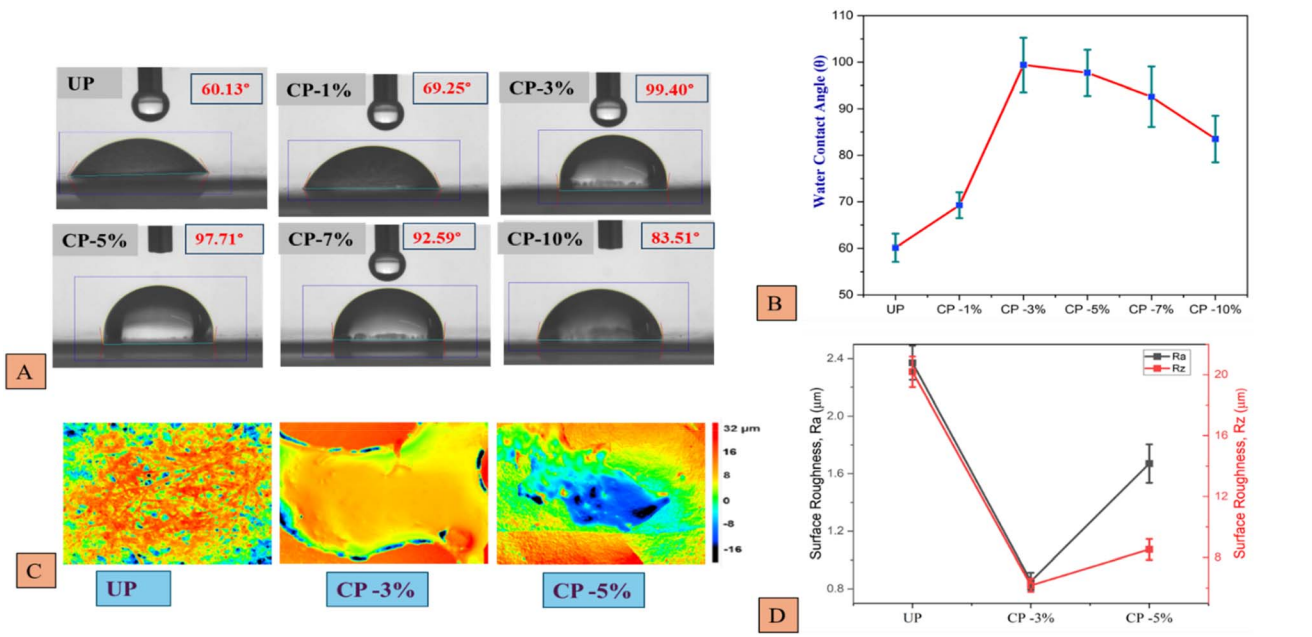

Fig. 8 (A) WCA of uncoated base paper and coated papers. (B) Change in the WCA of uncoated base paper and coated papers. (C) Surface profile of uncoated base paper and CP-3% and CP-5%. (D) Change in the surface roughness of uncoated base paper and CP-3% and CP-5%.

collagen hydrolysate, as it covers the porous structure of the cellulosic matrix throughout the uniform coating of the paper, which significantly increased water repellency. However, the WCA of CP-5%, CP-7% and CP-10% gradually decreased to 97.71°, 92.59° and 83.51°. As the concentration of CNCs increased, the presence of more surface hydroxyl groups reduced the contact angle. Fig. 8D illustrates how surface roughness was reduced with a uniform coating of CNCs and

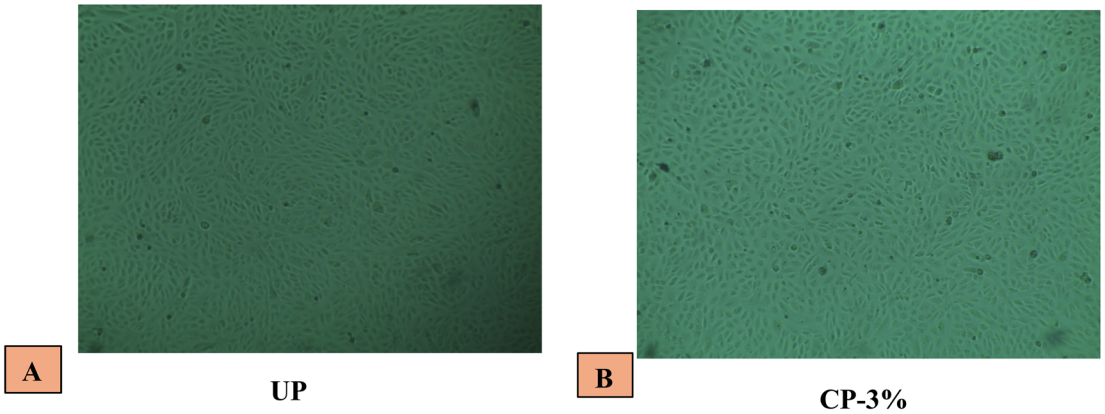

Fig. 9 Cytotoxic effect assessment of (A) uncoated base paper and (B) coated paper sample (CP-3%) using water as the solvent.

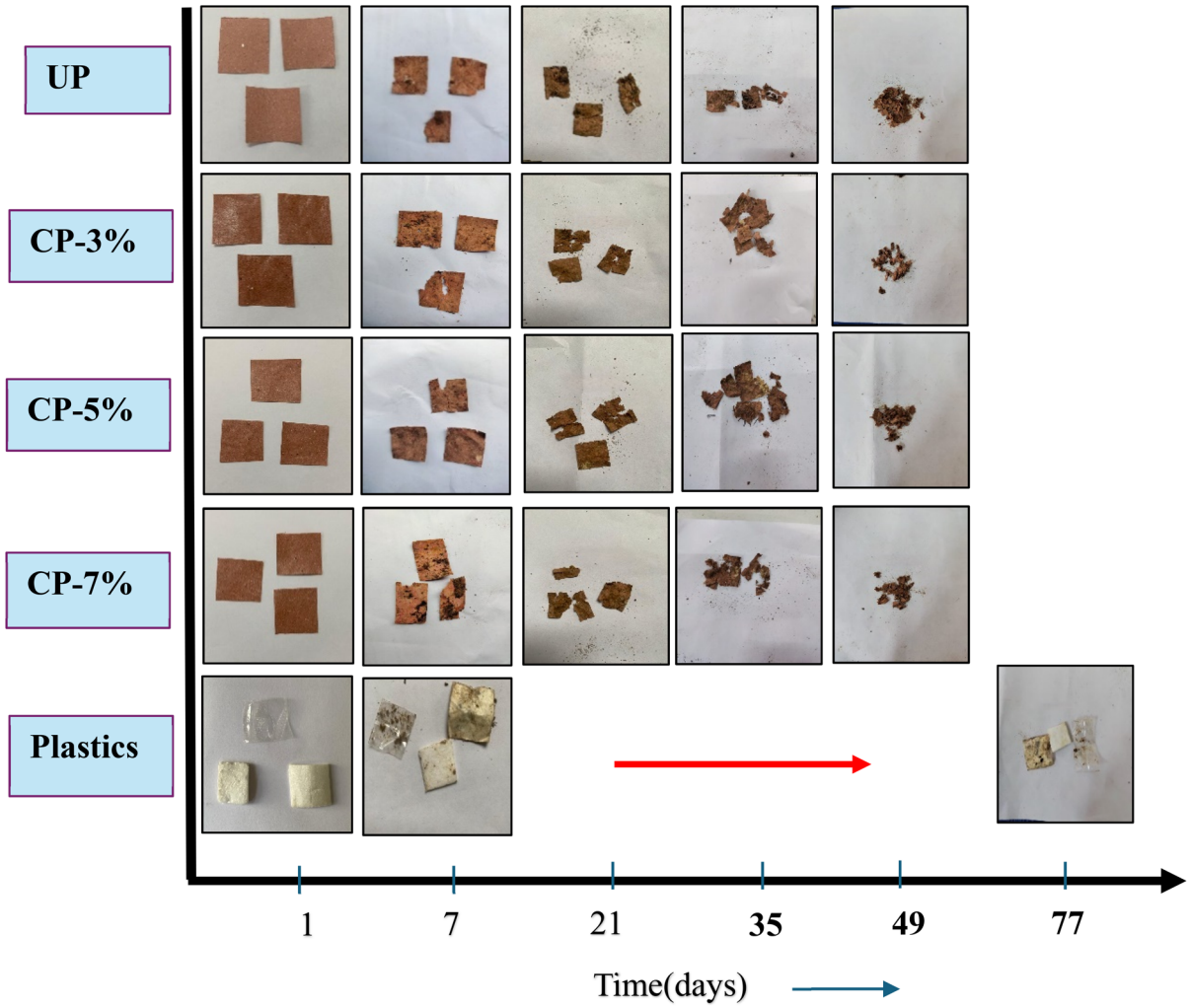

Fig. 10 Biodegradation of uncoated base paper, coated paper, and plastic materials.

collagen hydrolysate nanoparticles due to the uniform distribution of coating layers, which filled the gaps in the cellulose fiber matrix. As the WCA values gradually decreased in the case of CP-5%, CP-7%, and CP-10%, only CP-3% and CP-5% were considered for surface roughness tests. The non-uniform coating of CP-5% due to the agglomeration of CNCs at increased concentrations resulted in an uneven distribution of cellulose nanoparticles, thereby enhancing the surface roughness. Uniform coating resulted in a reduction of both average surface roughness and average roughness depth. Among them, CP-3% showed the best results, as shown in Fig. 8D.

A cytotoxicity assessment of the UP (control) and paper-coated CP-3% samples was conducted. The tested papers were found to be non-toxic when the test was conducted using a Vero cell line for DMEM (Dulbecco's modified Eagle's medium) in Fig. 9B. Direct contact with the UP and CP-3% resulted in cell viability of more than 95% after 48 h of incubation. No toxic effect was found in the coated papers. Cells were found to be alive, indicating no cytotoxic effect. Therefore, the paper could be used as a packaging material for food.

The biodegradability of plastics (polyethylene and polystyrene), uncoated base paper (UP), and coated papers was assessed using a soil burial test.[5,37] The results of the soil degradation test are depicted in Fig. 10. The UP sample and coated paper samples (CP-3%, CP-5%, and CP-7%) took almost 7 weeks to degrade fully. The coating did not delay the biodegradability of the paper samples by enhancing the barrier and physical properties. However, plastic samples were not changed after 11 weeks because microorganisms cannot quickly degrade synthetic polymers.

4 Conclusions

The application of CNCs, extracted from MOW, collagen hydrolysate, and glycerin on a paper substrate, introduced a new pathway for the development of bio-based coating applications. The crystallinity index of CNCs was around 87%, and the average length and diameter were approximately 104.08 $\pm$ 0.1 nm and 9.49 $\pm$ 0.3 nm, respectively. The modification was confirmed by the presence of FTIR peaks at 1096 cm^{-1} and 1020 cm^{-1}, which ensured the hydrogen bonding between the –OH group of cellulose and the $-NH_2$ and –COOH groups of collagen hydrolysate. FE-SEM images were acquired to investigate the surface morphology of the uncoated and coated samples, revealing a uniform coating on the surface of CP-3%. The barrier tests were conducted, and all coated paper samples passed; however, the uncoated paper failed in both the KIT and hot oil barrier tests. The water vapor resistance and air resistance of CP-3% increased by 14 times and 250 times, respectively, compared to the uncoated base paper, due to the uniform coating. The tensile index and burst index of CP-3% increased by 5.28 times and 1.79 times, respectively, compared to the uncoated paper. The water contact angle of the sample CP-3% increased by 39%, and the surface roughness decreased by 64.02%. No cytotoxic effect was observed in the CP-3% sample, with more than 95% of cells surviving. All the uncoated and coated paper samples took almost 77 days to fully degrade, whereas plastics such as polyethylene and polystyrene did not degrade. All the results proved that the CP-3% sample was highly suitable for packaging applications.

Ethical statement

The cytotoxic study was conducted in strict accordance with the Guidelines for the Care and Use of Laboratory Animals of the Centre for Advanced Research in Sciences at the University of Dhaka, utilizing their commercial services. The experimental procedures were approved by the Committee on the Ethics of Animal Experiments of the Centre for Advanced Research in Sciences at the University of Dhaka. In brief, Vero (a kidney cell line from an African green monkey) was kindly provided by Professor H. Hoshino (Gunma University Graduate School of Medicine, Gunma, Japan) and maintained in DMEM (Dulbecco's modified Eagle's medium) containing 1% penicillin–streptomycin (1 : 1), 0.2% gentamycin and 10% fetal bovine serum (FBS).

Data availability

The data supporting the findings of this study are available from the corresponding author upon reasonable request.

Author contributions

K. S. S. suggested the idea, designed the project, and secured the funding. A. B. and N. R. K. performed experiments and data analysis, prepared the figures, and wrote the manuscript. N. A. J. and M. I. H. E. performed the experiments, and M. B., M. M. R., A. F. M. M. R., M. R., L. P., and M. S. reviewed the manuscript. K. S. S. directed and monitored the research and reviewed and edited the manuscript. All authors significantly contributed to the writing of the manuscript.

Conflicts of interest

The authors declare that they have no conflict of interest.

Acknowledgements

This research was conducted in the Soft Materials Research Laboratory. Applied Chemistry and Chemical Engineering, University of Dhaka. The study of mechanical properties and water vapor permeability, and TGA were conducted at the Institute of Leather Engineering and Technology, University of Dhaka. The air permeability test was conducted at the Pulp and Paper Research Division (PPRD) of BCSIR, Dhaka. TEM, SEM, contact angle, and surface roughness tests were conducted in the Department of Forest Biomaterials at North Carolina State University. The authors acknowledge the funding support from the Grants for Advanced Research in Education (Project ID: ET-20222100), BANBEIS, Ministry of Education, Government of Bangladesh.

References

1 W. H. Danial, Z. Abdul Majid, M. N. Mohd Muhid, S. Triwahyono, M. B. Bakar and Z. Ramli, *Carbohydr. Polym.*, 2015, **118**, 165–169.
2 S. J. Risch, *J. Agric. Food Chem.*, 2009, **57**, 8089–8092.
3 I. Rahmawati, A. W. Pratama, S. A. Pratama, M. N. Khozin, A. Firmanda, F. H. Irawan, Asranudin, A. N. M. Ansori and T. H. Sucipto, *Case Stud. Chem. Environ. Eng.*, 2024, **10**, 100776, DOI: 10.1016/j.cscee.2024.100776.
4 L. K. Ncube, A. U. Ude, E. N. Ogunmuyiwa, R. Zulkifli and I. N. Beas, *Materials*, 2020, **13**, 4994.
5 K. S. Salem, M. Debnath, S. Agate, K. M. Y. Arafat, H. Jameel, L. Lucia and L. Pal, *Carbohydr. Polym. Technol. Appl.*, 2024, **7**, 100421.
6 M. M. A. Allouzi, D. Y. Y. Tang, K. W. Chew, J. Rinklebe, N. Bolan, S. M. A. Allouzi and P. L. Show, *Sci. Total Environ.*, 2021, **788**, 147815.
7 J. R. Jambeck, R. Geyer, C. Wilcox, T. R. Siegler, M. Perryman, A. Andrady, R. Narayan and K. L. Law, *Science*, 2015, **347**, 768–771.
8 M. Revel, A. Châtel and C. Mouneyrac, *Curr. Opin. Environ. Sci. Hlth.*, 2018, 17–23.
9 D. Biryol, C. I. Nicolas, J. Wambaugh, K. Phillips and K. Isaacs, *Environ. Int.*, 2017, **108**, 185–194.
10 J. N. Hahladakis, C. A. Velis, R. Weber, E. Iacovidou and P. Purnell, *J. Hazard. Mater.*, 2018, 179–199.
11 N. Evode, S. A. Qamar, M. Bilal, D. Barceló and H. M. N. Iqbal, *Case Stud. Chem. Environ. Eng.*, 2021, **4**, 100142.
12 D. Mahapatra, *J. Food Process Eng.*, 2024, 165–187.
13 P. Ezati, A. Khan, R. Priyadarshi, T. Bhattacharya, S. K. Tammina and J. W. Rhim, *Food Hydrocolloids*, 2023, 108771.
14 N. M. Stark and L. M. Matuana, *Mater. Today Sustain.*, 2021, **15**, 100084.
15 C. Andersson, *Packag. Technol. Sci.*, 2008, 339–373.
16 B. G. Hermann, L. Debeer, B. De Wilde, K. Blok and M. K. Patel, *Polym. Degrad. Stab.*, 2011, **96**, 1159–1171.
17 C. L. Reichert, E. Bugnicourt, M. B. Coltelli, P. Cinelli, A. Lazzeri, I. Canesi, F. Braca, B. M. Martínez, R. Alonso, L. Agostinis, S. Verstichel, L. Six, S. De Mets, E. C. Gómez, C. Ißbrücker, R. Geerinck, D. F. Nettleton, I. Campos, E. Sauter, P. Pieczyk and M. Schmid, *Polymers*, 2020, **12**, 1558.
18 C. Slaggert, *Kraft Heinz Online*, https://news.kraftheinzcompany.com/press-releases-details/2023/Kraft-Heinz-Announces-Goal-to-Reduce-the-Use-of-Virgin-Plastic-Globally-by-20-Percent–or-more-than-100-Million-Pounds–by-2030/default.aspx.
19 McDonald's Corporation, https://corporate.mcdonalds.com/corpmcd/our-stories/article/renewable_packaging.html.
20 V. Kumar, P. Pathak and N. K. Bhardwaj, *Waste Manag.*, 2021, **102**, 281–303, DOI: 10.1016/j.wasman.2019.10.041.
21 M. Debnath, K. S. Salem, V. Naithani, N. Starrett, E. Musten, M. A. Hubbe and L. Pal, in *TAPPICon 2023 – 'Rock the Roll: Unleashing the Harmonies of the Paper Industry'*, TAPPI Press, 2023.
22 P. Bajpai, in *Recycling and Deinking of Recovered Paper*, Elsevier, 2024, pp. 57–87.
23 A. Singh, L. M. Varghese, R. Dutt Yadav and R. Mahajan, *Environ. Sci. Pollut. Res.*, 2020, 45814–45823.
24 W. Wolska and E. Małachowska, *Forestry and Wood Technology*, 2023, 66–75.
25 M. Zubair, N. D. Mu'azu, M. Nasir, M. S. Manzar, M. A. Aziz, M. Saleem and M. A. Al-Harthi, *Arabian J. Sci. Eng.*, 2022, **47**, 5377–5393.
26 Y. Ikeda, E. Y. Park and N. Okuda, *Bioresour. Technol.*, 2006, **97**, 1030–1035.
27 H. Abushammala, M. A. Masood, S. T. Ghulam and J. Mao, *Sustainability*, 2023, **15**, 6915.
28 N. M. Stark, *J. Renewable Mater.*, 2016, **14**, 313–326.
29 A. J. Sayyed, D. V. Pinjari, S. H. Sonawane, B. A. Bhanvase, J. Sheikh and M. Sillanpää, *J. Environ. Chem. Eng.*, 2021, **9**, 106626.
30 T. Rusconi, L. Riva, C. Punta, M. Solé and I. Corsi, *Environ. Sci.: Nano*, 2024, **11**, 61–77.
31 T. Kovacs, V. Naish, B. O'Connor, C. Blaise, F. Gagné, L. Hall, V. Trudeau and P. Martel, *Nanotoxicology*, 2010, **4**, 255–270.
32 V. Dharini, A. Biswal, P. S. Sellamuthu, J. Jayaramudu and E. R. Sadiku, *Int. J. Food Sci. Technol.*, 2024, **59**, 318–332.
33 A. Ferrer, L. Pal and M. Hubbe, *Ind. Crops Prod.*, 2017, **95**, 574–582.
34 C. Amara, A. El Mahdi, R. Medimagh and K. Khwaldia, *Curr. Opin. Green Sustainable Chem.*, 2021, **31**, 100512.
35 S. S. Ahankari, A. R. Subhedar, S. S. Bhadauria and A. Dufresne, *Carbohydr. Polym.*, 2021, **255**, 117479.
36 S. S. Nair, J. Zhu, Y. Deng and A. J. Ragauskas, *Sustainable Chem. Processes*, 2014, **2**, 23.
37 N. A. Jashi, M. Debnath, L. Lucia, L. Pal, M. M. Rahman and K. S. Salem, *J. Polym. Environ.*, 2025, **33**, 1814–1828.
38 K. S. Salem, N. K. Kasera, M. A. Rahman, H. Jameel, Y. Habibi, S. J. Eichhorn, A. D. French, L. Pal and L. A. Lucia, *Chem. Soc. Rev.*, 2023, **52**, 6417–6446.
39 L. Segal, J. J. Creely, A. E. Martin and C. M. Conrad, *Text. Res. J.*, 1952, **29**, 43.
40 B. Deepa, E. Abraham, N. Cordeiro, M. Mozetic, A. P. Mathew, K. Oksman, M. Faria, S. Thomas and L. A. Pothan, *Cellulose*, 2015, **22**, 1075–1090.
41 K. S. Salem, H. R. Starkey, L. Pal, L. Lucia and H. Jameel, *ACS Sustain. Chem. Eng.*, 2020, **8**, 1471–1478.
42 P. Tyagi, L. A. Lucia, M. A. Hubbe and L. Pal, *Carbohydr. Polym.*, 2019, **206**, 281–288.
43 V. Muralidharan, M. S. Arokianathan, M. Balaraman and S. Palanivel, *Polym. Test.*, 2020, **81**, 106250.